

Table 1
Monosaccharide composition analysis by isotope-tag method

Glycoprotein	Monosaccharide	mol/mol ^a	mol/mol
Fetuin	Fuc	0.3	0 [20]
	Gal	10.4	12
	Man	7.6	9
	GlcNAc	14.7	15
	GalNAc	3.4	3
Erythropoietin	Fuc	3.4	4.1 [21]
	Gal	12.8	13.8
	Man	8.1	8.7
	GlcNAc	15.6	17.2
	GalNAc	1.5	0.9

^a Values were expressed as mol detected in 1 mol glycoprotein.

Fig. 4B, and F show the mass chromatograms of d₀-, and d₄-PA fucose, Fig. 4C and G indicate those of d₀-, d₄-PA hexose, and Fig. 4D and H show those of d₀-, d₄-PA HexNAc. The monosaccharide compositions of fetuin and erythropoietin calculated from the peak area ratios (d₀-PA/d₄-PA monosaccharides) were in good agreement with the reported values (Table 1) [20,21]. By heating the standard monosaccharides simultaneously the decomposition of monosaccharides during hydrolysis can be corrected, and a use of isotope analogs as the internal standards can reduce deviation in ESIMS analysis.

3.2. Quantitative oligosaccharide profiling using the isotope tag method

Next, we explored the capability of the isotope-tag method for the quantitative oligosaccharide profiling. When d₀-PA oligosaccharides prepared from an analyte glycoprotein are analyzed with an equal part of d₄-PA oligosaccharides prepared from a standard glycoprotein, oligosaccharides which link to both the analyte and the standard glycoproteins are expected to appear as paired ions with a difference of 4 Da, and the individual oligosaccharides in the analyte glycoprotein can be quantified based on the analyte/internal standard ion-pair intensity ratio. On the other hand, any oligosaccharides that link to either the analyte or the standard glycoprotein ought to be detected as single ions. Oligosaccharides released from rhCG and hCG were tagged with d₀- and d₆-AP, respectively, and the tagged oligosaccharides were analyzed by GCC-LC/MS in both positive and negative ion modes.

Fig. 5A and B show the mass spectra of the peak which was detected at 21.5 min in the positive and the negative ion mode, respectively. In the positive ion mode, ions at *m/z* 863.0, 1359.4 and 1197.2 were detected (Fig. 5A), and they can be assigned to d₄-PA [Hex]₅[HexNAc]₄²⁺ (an asialobiantennary oligosaccharide), d₄-PA[Hex]₃[HexNAc]₄⁺ (a fragment of the asialobiantennary form) and d₄-PA[Hex]₄[HexNAc]₄⁺ (a fragment of the asialobiantennary form), respectively. In contrast, only an ion at *m/z* 860.9 (d₄-PA[Hex]₅[HexNAc]₄²⁻, asialobiantennary oligosaccharide) was detected in the negative ion mode (Fig. 5B). This result suggests that mass spectra

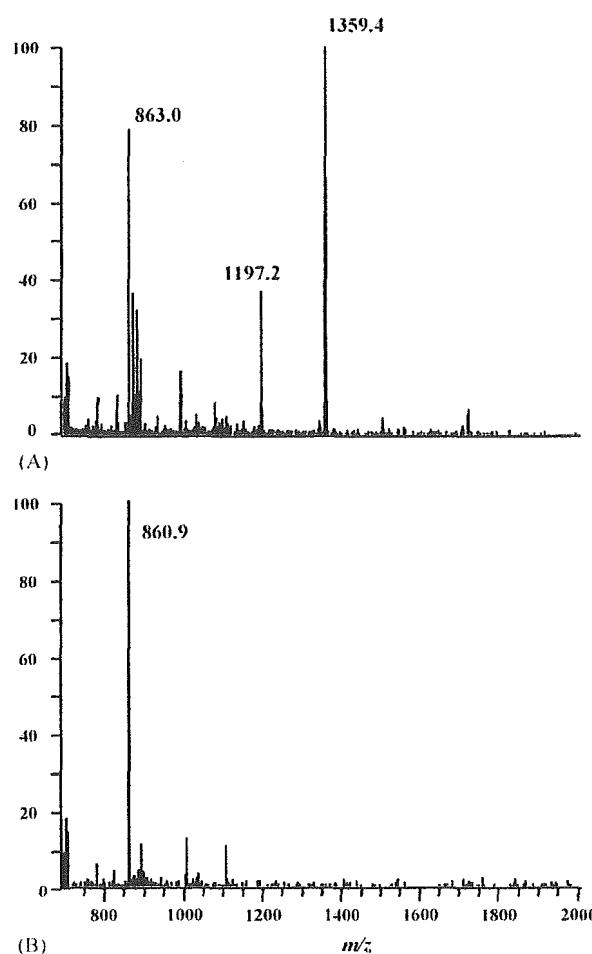


Fig. 5. Mass spectra of d₄-PA oligosaccharide. D₄-PA oligosaccharide eluted at 21.5 min from GCC was analyzed by ESIMS in the positive ion mode (A) and negative ion mode (B).

of PA oligosaccharides become complicated due to fragmentation in the positive ion mode, while only molecular ions can be detected in the negative ion mode. Therefore, ESI analysis in the negative ion mode was chosen for the PA oligosaccharide profiling.

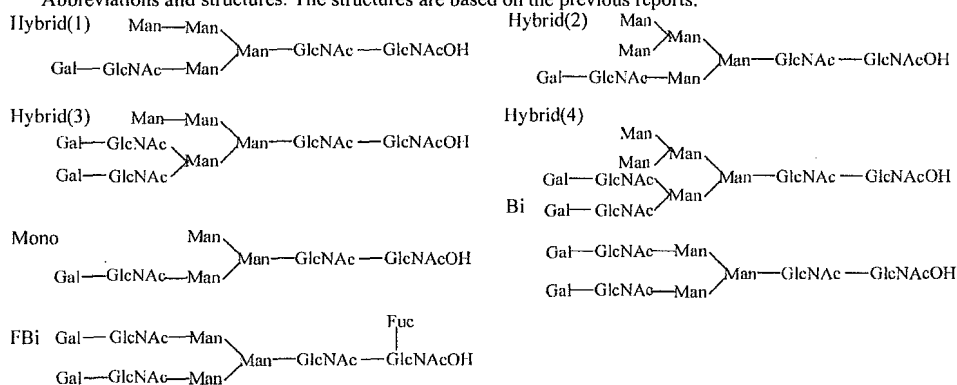
Fig. 6A and B show the TIC of a mixture of equal parts of d₀-PA oligosaccharides prepared from rhCG and d₄-PA oligosaccharides from hCG, and its two-dimensional display (retention time versus *m/z*), respectively. The carbohydrate structures, which can be deduced from *m/z* values, are indicated in Table 2. Paired ions at *m/z* 757.5, 759.5 were observed in the mass spectrum of peak a1. Based on carbohydrate composition [Hex]₅[HexNAc]₃, it can be assigned to a hybrid type oligosaccharide. Likewise, peak 11, 12, 14, 15, p1, p2, and p4 consisted of paired ions and can be assigned to monosialylated (11, 12, 14, 15) and disialylated (p1, p2) biantennary oligosaccharide without Fuc. Fig. 7 shows TIC of d₀-, d₄-PA oligosaccharides (A), extracted ion chromatograms of d₀-PA (B), d₄-PA (C), and d₀-, d₄-PA monosialylated biantennary form (D). The mass spectra of peaks 11–15 are shown in Fig. 7E–I. Peak 13 was not observed in Fig. 7D and only

Table 2
Structural assignment of peaks in Fig. 6B

Peak nos.	Carbohydrate composition ^a	Deduced structure ^b	Theoretical mass (d ₀ -PA-sugar)	Observed <i>m/z</i>			Ion-pair intensity ratio d ₀ /d ₄
				d ₀ -PA-rhCG		d ₄ -PA-hCG	
				M ²⁻	M ³⁻	M ²⁻	
a1	[Hex] ₅ [HexNAc] ₃	Hybrid (1)	1517.5	757.5		759.5	0.27
b1	[Hex] ₅ [HexNAc] ₄ [NeuNAc] ₂	Bi + NA ₂	2303.1			768.2	
c1	[Fuc] ₁ [Hex] ₅ [HexNAc] ₄ [NeuNAc] ₂	FBi + NA ₂	2449.3			816.7	
d1	[Hex] ₄ [HexNAc] ₃ [NeuNAc] ₁	Mono + NA	1646.6			824.3	
d2	[Hex] ₄ [HexNAc] ₃ [NeuNAc] ₁	Mono + NA	1646.6			824.0	
e1	[Hex] ₆ [HexNAc] ₃	Hybrid (2)	1679.6	838.6			
e2	[Hex] ₆ [HexNAc] ₃	Hybrid (2)	1679.6			840.6	
f1	[Hex] ₅ [HexNAc] ₄	Bi	1720.7	858.9			
f2	[Hex] ₅ [HexNAc] ₄	Bi	1720.7			861.2	
g1	[Hex] ₅ [HexNAc] ₃ [NeuNAc] ₁	Hybrid (1) + NA	1807.7	902.9			
g2	[Hex] ₅ [HexNAc] ₃ [NeuNAc] ₁	Hybrid (1) + NA	1808.7			905.0	
h1	[Fuc] ₁ [Hex] ₅ [HexNAc] ₄	FBi	1866.8			934.0	
i1	[Hex] ₆ [HexNAc] ₄	Hybrid (3)	1882.8	940.2			
j1	[Hex] ₅ [HexNAc] ₅	Bi + GN	1924.9			962.7	
k1	[Hex] ₆ [HexNAc] ₃ [NeuNAc] ₁	Hybrid (2) + NA	1970.8			986.8	
k2	[Hex] ₆ [HexNAc] ₃ [NeuNAc] ₁	Hybrid (2) + NA	1970.8			986.2	
l1	[Hex] ₅ [HexNAc] ₄ [NeuNAc] ₁	Bi + NA	2011.9	1004.7		1006.7	0.77
l2	[Hex] ₅ [HexNAc] ₄ [NeuNAc] ₁	Bi + NA	2011.9	1004.6		1007.3	0.56
l3	[Hex] ₅ [HexNAc] ₄ [NeuNAc] ₁	Bi + NA	2011.9	1004.6			
l4	[Hex] ₅ [HexNAc] ₄ [NeuNAc] ₁	Bi + NA	2011.9	1004.6		1006.5	0.67
l5	[Hex] ₅ [HexNAc] ₄ [NeuNAc] ₁	Bi + NA	2011.9	1004.6		1006.4	0.49
m1	[Hex] ₇ [HexNAc] ₄	Hybrid (4)	2044.9	1021.4			
n1	[Fuc] ₁ [Hex] ₅ [HexNAc] ₄ [NeuNAc] ₁	FBi + NA	2158.0			1079.8	
n2	[Fuc] ₁ [Hex] ₅ [HexNAc] ₄ [NeuNAc] ₁	FBi + NA	2158.0			1079.8	
n3	[Fuc] ₁ [Hex] ₅ [HexNAc] ₄ [NeuNAc] ₁	FBi + NA	2158.0			1079.8	
o1	[Hex] ₆ [HexNAc] ₄ [NeuNAc] ₁	Hybrid (3) + NA	2174.0	1085.6			
o2	[Hex] ₆ [HexNAc] ₄ [NeuNAc] ₁	Hybrid (3) + NA	2174.0	1085.7			
p1	[Hex] ₅ [HexNAc] ₄ [NeuNAc] ₂	Bi + NA ₂	2303.1	1150.3		1152.1	5.76
p2	[Hex] ₅ [HexNAc] ₄ [NeuNAc] ₂	Bi + NA ₂	2303.1	1150.2		1152.2	5.92
p3	[Hex] ₅ [HexNAc] ₄ [NeuNAc] ₂	Bi + NA ₂	2303.1	1150.1			
p4	[Hex] ₅ [HexNAc] ₄ [NeuNAc] ₂	Bi + NA ₂	2303.1	1150.3		1152.4	0.45

^a Hex, hexose; HexNAc, *N*-acetyl hexosamine; NeuNAc, *N*-acetyl neuraminic acid; Fuc, fucose.

^b Abbreviations and structures. The structures are based on the previous reports.



single ion was detected in Fig. 7G. These results suggest that one of monosialylated binantennary oligosaccharides isomers links to only rhCG.

We determined relative amounts of some oligosaccharides in rhCG on the basis of ion-pair intensity ratios (Table 2). The amount of monosialylated binantennary forms (l1, l2, l4, and l5) linked to rhCG were 50–70% of those to hCG. The amount of disialylated binantennary forms (p1 and p2) linked to rhCG

was five-fold of those to hCG, and the linkage of p4 to rhCG was one-half of that of hCG. The isotope tag method clearly shows the difference in distribution of isomers between rhCG and hCG.

In this procedure, oligosaccharides linked to either rhCG or hCG were detected as single ions. As shown in Table 2, nine oligosaccharides were detected as single ions in rhCG, and they are reduced to hybrid type and complex type.

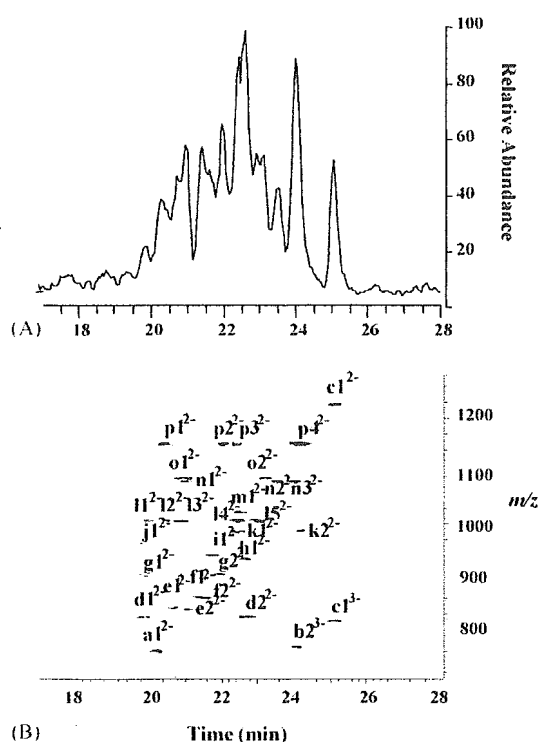


Fig. 6. TIC of a mixture of equal amount of d_0 -PA N-linked oligosaccharides from rhCG and d_4 -PA N-linked oligosaccharides from hCG (A), and its 2D display (B). Oligosaccharides (from 2 μ g rhCG and hCG) were analyzed by GCC-LC/MS in the negative ion mode.

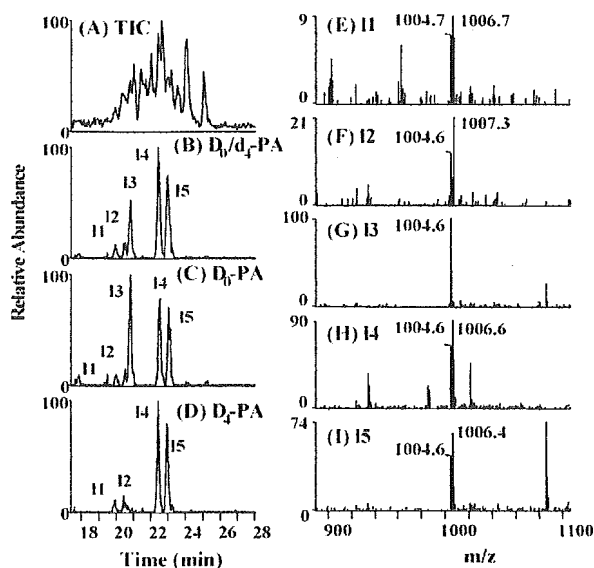


Fig. 7. TIC of a mixture of equal amount of d_0 -PA N-linked oligosaccharides from rhCG and d_4 -PA N-linked oligosaccharides from hCG (A). Extracted ion chromatograms of d_0 - and d_4 -PA monosialylated biantennary (set m/z values, 1004–1007) (B), d_0 -PA monosialylated biantennary (set m/z values, 1004–1005) (C), and d_4 -PA monosialylated biantennary oligosaccharides (set m/z values, 1006–1007) (D). Mass spectra of peak 11–15 (E–I).

Fourteen oligosaccharides were detected only in hCG, and most of them were fucosylated complex type. These results show the differences in glycosylation between rhCG and hCG and suggest that many hybrid type oligosaccharides linked to rhCG, while fucosylated oligosaccharides attach to hCG.

4. Discussion

Alteration of glycosylation is known to cause many changes in the biological activity as well as the physical properties of proteins. Several procedures of oligosaccharide profiling have been reported for the assessment of alteration of glycosylation, however, most of them can be used for only either qualitative or quantitative analysis. Although mass spectrometric oligosaccharide profiling is useful for the qualitative analysis, it has a problem on precision, and some isomers are still indistinguishable if their retention times are closed to others. In this study, we demonstrated that the use of isotope-tagged internal standards and GCC-LC/MS made it possible to do both quantitative and qualitative carbohydrate analysis.

First, we demonstrated the monosaccharide composition analysis using the isotope tag method. The use of internal standards that were heated under the same hydrolysis condition as an analyte glycoprotein resulted in good precision and accuracy in the monosaccharide composition analysis. Several HPLC methods for determination of monosaccharides have been reported. High-performance anion-exchange chromatography with pulsed amperometric detection (HPAEC-PAD) has been widely used for monosaccharide composition analysis [20,22–25]. Although HPAEC-PAD gives high resolution of all common monosaccharides and has the advantage of not requiring derivatization, this method is also known to have a disadvantage of limited selectivity [26]. The isotope tag method with SIM mode is equal to the HPAEC-PAD in sensitivity and is better than it in selectivity.

Next, we demonstrated the potentiality of the isotope tag method for quantitative oligosaccharide profiling using rhCG and hCG as model glycoproteins. hCG consists of an α subunit (MW 14.7 kDa) and a β subunit (MW 23.0 kDa), and oligosaccharides link to Asn52, and 78 in the α subunit and Asn13 and 30 in the β subunit. It has been reported that the majority of N-linked oligosaccharides in rhCG and hCG are fucosylated or non-fucosylated di-, tri-, and tetra-antennary forms with a various level of sialylation [27–30]. We prepared d_0 -PA oligosaccharides and d_4 -PA oligosaccharides from rhCG and hCG, respectively, and an equal part of d_0 -PA and d_4 -PA oligosaccharides was injected into LC/MS. We demonstrated that the oligosaccharides existing in one side protein were detected as single ions, whereas common oligosaccharides were detected as paired ions. We could easily realize that monosialo-, and disialobiantennary oligosaccharides linked to both hCG and rhCG, while fucosylated oligosaccharides and some hybrid type oligosaccharides linked to only hCG and rhCG, respectively. In addition, we demonstrated the pos-

sibility of the quantitative comparison the oligosaccharides between two quite similar glycoproteins. This quantitative oligosaccharide profiling is expected to be a powerful tool in various stages, including quality control and comparability assessment of glycoprotein products, and elucidation of glycan alteration in some diseases.

Acknowledgements

This study was supported in part by the Japan–China Sasakawa Medical Fellowship (J.Y.) and by a grant-in-aid for Research on Health Sciences focusing on Drug Innovation from The Japan Health Sciences Foundation (N.K.).

References

- [1] A. Varki, *Glycobiology* 3 (1993) 97.
- [2] T. Hayakawa, in: Y.-y.H. Chiu, J.L. Gueriguian (Eds.), *Drug Biotechnology Regulation. Scientific Basis and Practices*, Marcel Dekker Inc., New York, 1991, p. 468.
- [3] N. Takahashi, H. Nakagawa, K. Fujikawa, Y. Kawamura, N. Tomiya, *Anal. Biochem.* 226 (1995) 139.
- [4] R.R. Townsend, M.R. Hardy, O. Hindsgaul, Y.C. Lee, *Anal. Biochem.* 174 (1988) 459.
- [5] G.R. Guile, P.M. Rudd, D.R. Wing, S.B. Prime, R.A. Dwek, *Anal. Biochem.* 240 (1996) 210.
- [6] L. Royle, T.S. Mattu, E. Hart, J.I. Langridge, A.H. Merry, N. Murphy, D.J. Harvey, R.A. Dwek, P.M. Rudd, *Anal. Biochem.* 304 (2002) 70.
- [7] J. Delaney, P. Vouros, *Rapid Commun. Mass Spectrom.* 15 (2001) 325.
- [8] K.A. Thomsson, H. Karlsson, G.C. Hansson, *Anal. Chem.* 72 (2000) 4543.
- [9] N. Kawasaki, M. Ohta, S. Hyuga, M. Hyuga, T. Hayakawa, *Anal. Biochem.* 285 (2000) 82.
- [10] N. Kawasaki, S. Itoh, M. Ohta, T. Hayakawa, *Anal. Biochem.* 316 (2003) 15.
- [11] N. Kawasaki, M. Ohta, S. Itoh, M. Hyuga, S. Hyuga, T. Hayakawa, *Biologicals* 30 (2002) 113.
- [12] S.P. Gygi, B. Rist, S.A. Gerber, F. Turecek, M.H. Gelb, R. Aebersold, *Nat. Biotechnol.* 17 (1999) 994.
- [13] S. Hase, T. Ikenaka, Y. Matsushima, *Biochem. Biophys. Res. Commun.* 85 (1978) 257.
- [14] S. Hase, S. Hara, Y. Matsushima, *J. Biochem. (Tokyo)* 85 (1979) 217.
- [15] S. Suzuki, K. Takehi, S. Honda, *Anal. Chem.* 68 (1996) 2073.
- [16] M. Wuhrer, H. Geyer, M. von der Ohe, R. Gerardy-Schahn, M. Schachner, R. Geyer, *Biochimie* 85 (2003) 207.
- [17] S. Itoh, N. Kawasaki, M. Ohta, T. Hayakawa, *J. Chromatogr. A* 978 (2002) 141.
- [18] J.Q. Fan, Y. Namiki, K. Matsuoka, Y.C. Lee, *Anal. Biochem.* 219 (1994) 375.
- [19] H. Takemoto, S. Hase, T. Ikenaka, *Anal. Biochem.* 145 (1985) 245.
- [20] M.R. Hardy, R.R. Townsend, Y.C. Lee, *Anal. Biochem.* 170 (1988) 54.
- [21] H. Sasaki, B. Bothner, A. Dell, M. Fukuda, *J. Biol. Chem.* 262 (1987) 12059.
- [22] M.R. Hardy, *Methods Enzymol.* 179 (1989) 76.
- [23] C.C. Ip, V. Manam, R. Hepler, J.P. Hennessey Jr., *Anal. Biochem.* 201 (1992) 343.
- [24] A. Lampio, J. Finne, *Anal. Biochem.* 197 (1991) 132.
- [25] Y.C. Lee, *Anal. Biochem.* 189 (1990) 151.
- [26] M. Weitzhandler, C. Pohl, J. Rohrer, L. Narayanan, R. Slingsby, N. Avdalovic, *Anal. Biochem.* 241 (1996) 128.
- [27] A. Kobata, *J. Cell Biochem.* 37 (1988) 79.
- [28] Y. Endo, K. Yamashita, Y. Tachibana, S. Tojo, A. Kobata, *J. Biochem. (Tokyo)* 85 (1979) 669.
- [29] A. Amoresano, R. Siciliano, S. Orru, R. Napoleoni, V. Altarocca, E. De Luca, A. Sirna, P. Pucci, *Eur. J. Biochem.* 242 (1996) 608.
- [30] A. Gervais, Y.A. Hammel, S. Pelloux, P. Lepage, G. Baer, N. Carte, O. Sorokine, J.M. Strub, R. Koerner, E. Leize, A. Van Dorsselaer, *Glycobiology* 13 (2003) 179.

Specific detection of Lewis x-carbohydrates in biological samples using liquid chromatography/multiple-stage tandem mass spectrometry

Noritaka Hashii^{1,2}, Nana Kawasaki^{1,2*}, Satsuki Itoh¹, Akira Harazono¹, Yukari Matsuishi^{1,2}, Takao Hayakawa³ and Toru Kawanishi¹

¹Division of Biological Chemistry and Biologicals, National Institute of Health Sciences, 1-18-1 Kamiyoga, Setagaya-ku, Tokyo 158-8501, Japan

²Core Research for Evolutional Science and Technology (CREST) of Japan Science and Technology Agency (JST), Kawaguchi Center Building, 4-1-8 Hon-cho, Kawaguchi, Saitama 332-0012, Japan

³Pharmaceutical and Medical Devices Agency, 3-3-2 Kasumigaseki, Chiyoda-ku, Tokyo 100-0013, Japan

Received 14 July 2005; Revised 5 September 2005; Accepted 8 September 2005

The Lewis x structure [Le^x, Gal β 1-4(Fuc α 1-3)GlcNAc] motif is one of the tumor antigens and plays an important role in oncogenesis, development, cellular differentiation and adhesion. The detection of Le^x-carbohydrates and their structural analysis are necessary to clarify the role of Le^x in several biological events. Mass spectrometry has been preferably used for the structural analysis of carbohydrates. Especially, collision-induced dissociation (CID) tandem mass spectrometry (MS/MS), which causes a glycosidic bond cleavage, is used for carbohydrate sequencing. However, Le^x cannot be identified by MS/MS due to the existence of the positional isomers, such as Lewis a [Gal β 1-3(α 1-4Fuc)GlcNAc]. In the present study, we demonstrate the specific detection of Le^x-carbohydrates in a biological sample by using multiple-stage MS/MS (MSⁿ). Using pyridylaminated oligosaccharides bearing Le^x, we found that the Le^x-motif yields a cross-ring fragment by the cleavage of a bond between C-3 and C-4 of GlcNAc in Gal(Fuc)GlcNAc. The Le^x-specific cross-ring fragment ion at *m/z* 259 was effectively detected by sequential scans, consisting of a full MS¹ scan, data-dependent CID MS² scan, MS³ of [Gal(Fuc)GlcNAc+Na]⁺ at *m/z* 534, and MS⁴ of [GalGlcNAc+Na]⁺ at *m/z* 388. The sequential scan was applied to *N*-linked oligosaccharide profiling using a LC/ESI-MSⁿ system equipped with a graphitized carbon column. We successfully detected the Le^x-motif and elucidated the structures of several Le^x and Lewis y [(Fuc α 1-2)Gal β 1-4(Fuc α 1-3)GlcNAc] oligosaccharides in the murine kidney used as a model tissue. Our method is expected to be a powerful tool for the specific detection of the Le^x-motif, and structural elucidation of Le^x-carbohydrates in biological samples. Copyright © 2005 John Wiley & Sons, Ltd.

The Lewis x structure [Le^x, Gal β 1-4(Fuc α 1-3)GlcNAc] is one of the tumor antigens, and plays an important role in oncogenesis^{1,2} (abbreviations used here are: Gal, galactose; Fuc, fucose; GlcNAc, *N*-acetylglucosamine). Particularly, sialylated Le^x is used as a marker of lung, pancreas and uterus tumors.³ Le^x and its derivatives are also known to be oligosaccharide ligands of some endothelial receptors, such as the selectins and the scavenger receptor, C-type lectin,^{4,5} and affect embryonic development, cellular differentiation and adhesion.^{6,7} However, the structural details of the oligosaccharides attached to the Le^x structure (Le^x-oligosaccharide) are still unclear. Le^x structure-specific detection and elucidation

methods are necessary for the diagnosis of tumors and a study on the role of Le^x on various biological events.

Mass spectrometry (MS) has become very popular for the structural analysis of oligosaccharides. Low-energy collision-induced dissociation (CID) tandem mass spectrometry (MS/MS), which generates B/Y-series ions by glycosidic bond cleavage, is preferably used for oligosaccharide sequencing.^{8–13} However, the detection of Le^x by MS/MS is still challenging due to the presence of its positional isomer, Lewis a [Le^a, Gal β 1-3(Fuc α 1-4)GlcNAc]. The structural difference between Le^x and Le^a is the linkage at positions 3 or 4 of the non-reducing terminal fucose and galactose to GlcNAc (Fig. 1). For the linkage analysis, multiple-stage MS/MS (MSⁿ) pattern-matching, in which the oligosaccharide structure can be deduced from intensity ratios of fragment ions generated by MSⁿ, has recently been reported;^{14–16} however, this method needs an identical analytical condition and various oligosaccharide standards. As an alternative method, the cross-ring fragmentation caused by MSⁿ is

*Correspondence to: N. Kawasaki, Division of Biological Chemistry and Biologicals, National Institute of Health Sciences, 1-18-1 Kamiyoga, Setagaya-ku, Tokyo 158-8501, Japan.

E-mail: nana@nihs.go.jp

Contract/grant sponsor: Ministry of Health Labor and Welfare, and Core Research for the Evolutional Science and Technology Program, Japan Science and Technology Corp.

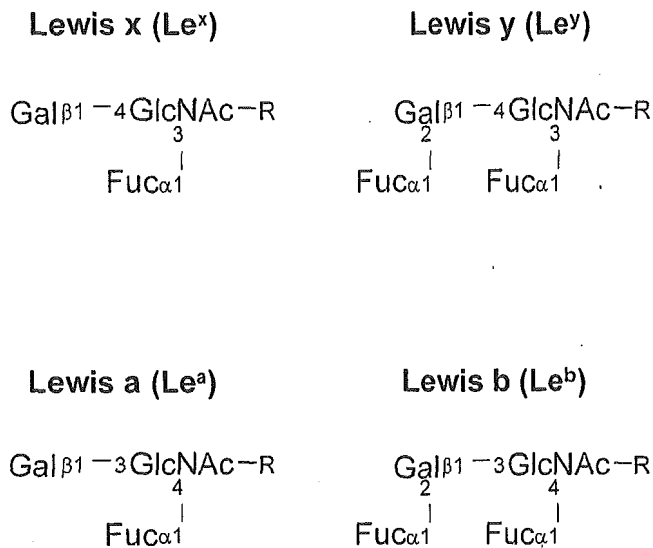


Figure 1. Structures of Lewis a, b, x and y.

sometimes used.^{10,17,18} Meisen *et al.*¹⁹ demonstrated that α 2-6-linked *N*-acetylneuraminic acid (NeuNAc) can be distinguished from α 2-3-linked NeuNAc based on structure-specific cross-ring fragment ions generated by low-energy CID MS² in the negative ion mode. Le^x could be expected to be distinguished from its positional isomers by cross-ring fragmentation.

In this study, we demonstrate the specific detection of Le^x-carbohydrates in a biological sample by using MSⁿ. Using pyridylaminated oligosaccharides bearing Le^x, we found that the Le^x-motif yields a cross-ring fragment by the cleavage of a bond between C-3 and C-4 of GlcNAc in Gal(Fuc)GlcNAc. The Le^x-specific cross-ring fragment ion at *m/z* 259 was effectively detected by sequential scans, consisting of a full MS¹ scan, data-dependent CID MS² scan, MS³ of [Gal(Fuc)GlcNAc+Na]⁺ at *m/z* 534, and MS⁴ of [GalGlcNAc+Na]⁺ at *m/z* 388 using nano-electrospray ionization-ion trap mass spectrometry (nanoESI-ITMS) in positive ion mode. Then, sequential MS¹⁻⁴ scanning for the Le^x-characteristic ions was applied for *N*-linked oligosaccharide profiling using an LC/ESI-ITMS instrument equipped with a graphitized carbon column (GCC), by which diverse oligosaccharides, including isomers, can be separated. We successfully detected the Le^x-motif and subsequently elucidated the entire structure of Le^x-oligosaccharides in the model tissue, murine kidney, in which Le^x-oligosaccharides are abundantly present.²⁰

EXPERIMENTAL

Materials

2-Aminopyridine (PA)-labeled pentasaccharides bearing Le^x (oligosaccharide I, Fig. 2(A)) or Le^a (oligosaccharide II, Fig. 2(B)), and the asialotriantennary oligosaccharide bearing Le^x (oligosaccharide III, Fig. 2(C)), were purchased from Takara Biomedicals (Otsu, Japan). Murine kidneys (MRL/MpJ-+/+) were purchased from Japan SLC Inc. (Hamamatsu, Japan).

Sample preparation

Proteins from murine kidneys were solubilized in lysis buffer (7 M urea, 2 M thiourea, 2% CHAPS, 30 mM Tris-HCl) by vor-

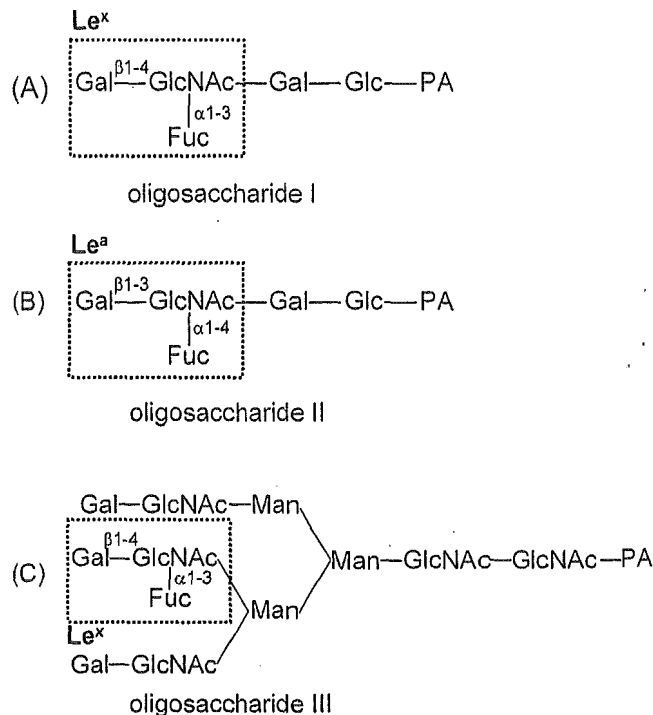


Figure 2. Structures of model oligosaccharides used in this study: (A) PA-labeled Le^x-pentasaccharide (oligosaccharide I); (B) PA-labeled Le^a-pentasaccharide (oligosaccharide II); and (C) PA-labeled Le^x-asialotriantennary complex type oligosaccharide (oligosaccharide III).

texting at room temperature. The proteins (100 μ g) were recovered by precipitation in cold acetone, and then treated with 10 units of PNGase F in 500 μ L of 0.2 M phosphate buffer (pH 7.6) at 37°C for 48 h to release the *N*-linked oligosaccharides. Proteins were removed by precipitation in cold ethanol, and the supernatant containing oligosaccharides was evaporated and lyophilized. The dried oligosaccharides were labeled with PA according to a previous report.²¹ The PA-labeled oligosaccharides were desalted with Envi-Carb C (Supelco Bellefonte, USA) and lyophilized.

nanoESI-MSⁿ

Experiments were performed using a Finnigan linear ion trap Fourier transform ion cyclotron resonance mass spectrometer (LTQ-FT, ThermoElectron, San Jose, CA, USA) equipped with a nanoESI source (AMR, Inc., Tokyo, Japan). ESI-MSⁿ was carried out for Le^x- and Le^a-oligosaccharide standards at a concentration of 1 pmol/ μ L in 5 mM ammonium acetate and 10 μ M NaCl buffer (pH 9.6) containing 50% acetonitrile. The sample was analyzed at a flow rate of 2.0 μ L/min using a spray voltage of 2.0 kV in the positive ion mode. The capillary temperature was set to 200°C; collision energies were set to 20–30% for the MSⁿ experiments; the maximum scan time was set to 50 ms. MS² and MS³ were performed with an isolation width of 3.0 u (range of precursor ion \pm 1.5).

LC/MSⁿ

LC was carried out using a MAGIC 2002 system (Michrom BioResources, Auburn, CA, USA) equipped with a GCC (Hypercarb column, 150 \times 0.2 mm, ThermoElectron). The

eluent were 5 mM ammonium acetate, pH 9.6, containing 2% acetonitrile (pump A) and 5 mM ammonium acetate, pH 9.6, containing 80% acetonitrile (pump B). PA-labeled *N*-linked oligosaccharides from murine kidney were eluted at a flow rate of 2 μ L/min with a gradient of 10–70% of pump B in 60 min. A solution of NaCl (10 μ M) was passed post-column at a flow rate of 2 μ L/min. The precursor ions detected by a full MS¹ scan (mass range at m/z 750–2000) were followed by MS² scans of the most intense ions.

RESULTS AND DISCUSSION

MSⁿ of Le^x-pentaoligosaccharide

The model Le^x-pentaoligosaccharide (oligosaccharide I) was analyzed by nanoESI-MSⁿ with direct injection in the positive ion mode. Sodium chloride (NaCl) was deliberately added to the sample for the acceleration of the cross-ring cleavages according to previous reports.^{22–24} The sodiated singly charged molecular ion, [M+Na]⁺, of oligosaccharide I was observed at m/z 954.4 in the MS¹ spectrum (Fig. 3(A)). MS² of the sodiated molecular ion yielded [(M+Na)-Fuc]⁺ at m/z 808 as the most intense ion by the glycosidic bond cleavage between GlcNAc and Fuc residues (Fig. 3(B)). This indicates that the Fuc residue is easily dissociated by low-energy CID MS². In addition to the defucosylated ions, we observed the sodiated ion at m/z 534, corresponding to the Le^x and Le^a structure, [Gal(Fuc)GlcNAc+Na]⁺. The sodiated B₂ ion (m/z 534) was subjected to a further product ion scan, and the sodiated ion at m/z 388 corresponding to [GalGlcNAc+Na]⁺ appeared in the MS³ spectrum (Fig. 3(C)). The ion at m/z 372, corresponding to [FucGlcNAc+Na]⁺, which proves the attachment of Fuc to GlcNAc, was also detected. Then, MS⁴

of the sodiated Y_{3 α} ion (m/z 388) yielded a sodiated cross-ring fragment ion at m/z 259, corresponding to the sodiated ^{3,5}A₂ ion, which proves the linkage of the Gal residue at position C-4 on GlcNAc, with some neutral losses: 60 Da (^{0,4}A₂, ^{0,4}X_{4 β} , ^{1,3}X_{4 β} and ^{2,4}X_{4 β}) and 90 Da (^{0,3}X_{4 β} and ^{1,4}X_{4 β}) (Fig. 3(D)).

MSⁿ of Le^a-pentaoligosaccharide

The Le^a-pentasaccharide (oligosaccharide II) was subjected to nanoESI-MSⁿ in a similar manner. The [M+Na]⁺ of oligosaccharide II was observed at m/z 954.4 in the MS¹ spectrum (Fig. 4(A)). MS² of the [M+Na]⁺ at m/z 954 yielded the sodiated ion at m/z 534, corresponding to [Gal(Fuc)GlcNAc+Na]⁺ (Fig. 4(B)). MS³ of the sodiated B₂ ion (m/z 534) yielded the sodiated Y_{3 α} and Y_{3 β} ions at m/z 372 and 388, respectively (Fig. 4(C)). MS⁴ of the sodiated Y_{3 β} ion at m/z 388 yielded some cross-ring fragment ions at m/z 208, 268, 298 and 328, corresponding to neutral losses: 60 Da (^{0,4}A₂, ^{0,4}X_{4 β} , ^{1,3}X_{4 β} and ^{2,4}X_{4 β}) and 90 Da (^{0,3}A₂, ^{0,3}X_{4 β} and ^{1,4}X_{4 β}) (Fig. 4(D)). ^{3,5}A₂ at m/z 259, which arose from oligosaccharide I, was not detected by MS⁴ of Le^a.

These results suggest that the Le^x structure can be identified by the ^{3,5}A₂ ion at m/z 259 generated by MS⁴ of [GalGlcNAc+Na]⁺ at m/z 388, which arose from MS³ [Gal(Fuc)GlcNAc+Na]⁺ at m/z 534 (Fig. 5).

MSⁿ of Le^x-asialotriantennary oligosaccharide

Using a Le^x-oligosaccharide with a more complicated branching structure, we confirmed the practicability of MS³ of the ion at m/z 534 followed by MS⁴ of the ion at m/z 388 for the detection of the Le^x-diagnostic ion at m/z 259.

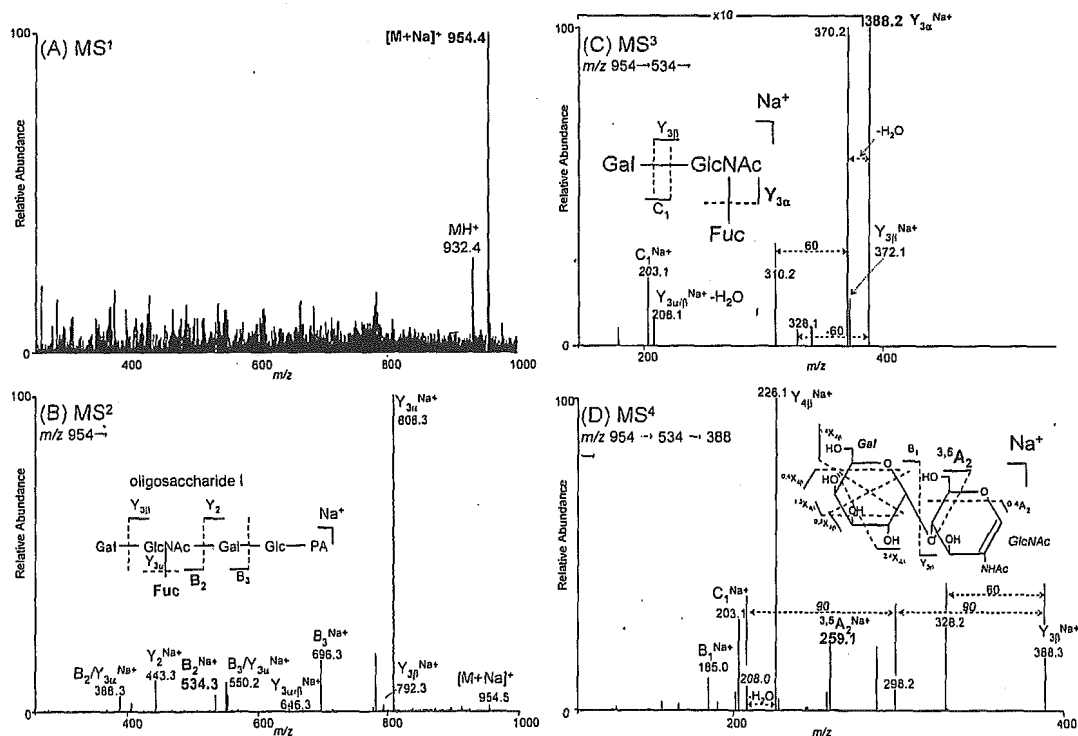


Figure 3. MS^{1–4} spectra of oligosaccharide I by ESI-MSⁿ: (A) MS¹ spectrum; (B) MS² spectrum of [M+Na]⁺ at m/z 954.4; (C) MS³ spectrum of [Gal(Fuc)GlcNAc+Na]⁺ at m/z 534.3 detected in MS²; and (D) MS⁴ spectrum of [GalGlcNAc+Na]⁺ at m/z 388.2 detected in MS³.

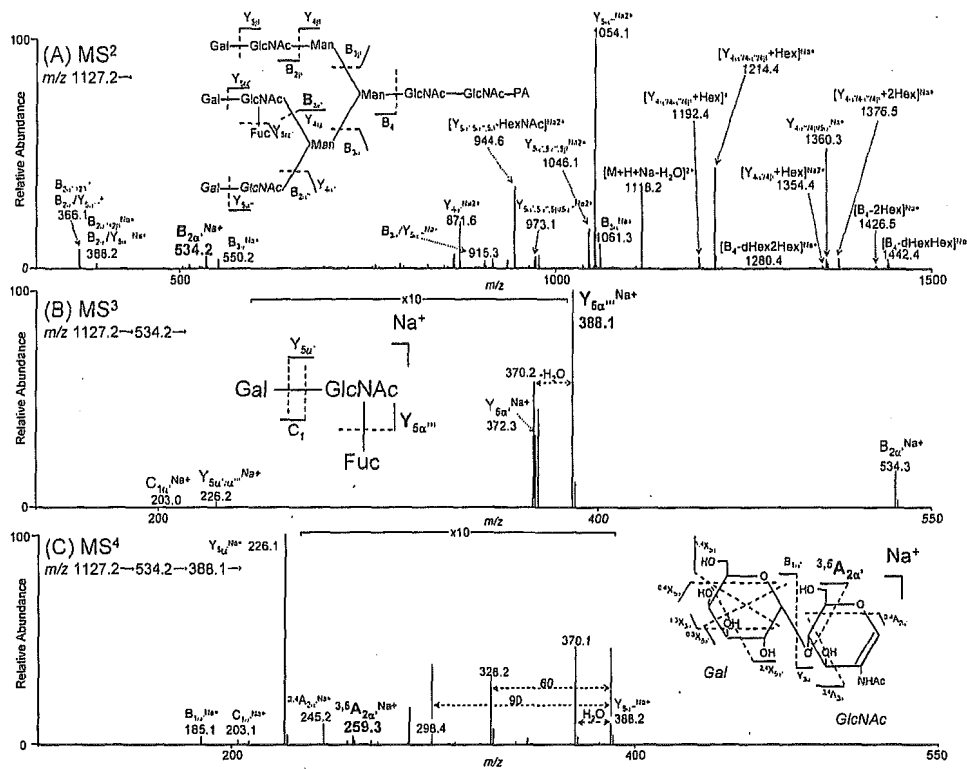


Figure 6. MS²⁻⁴ spectra of oligosaccharide III by ESI-MSⁿ: (A) MS² spectrum of [M+H+Na]²⁺ at *m/z* 1127.2; (B) MS³ spectrum of [Gal(Fuc)GlcNAc+Na]⁺ at *m/z* 534.2 detected in MS²; and (C) MS⁴ spectrum of [GalGlcNAc+Na]⁺ at *m/z* 388.1 detected in MS³.

diagnostic ions by MS¹⁻⁴ scans were presumed to be those of Le^x-oligosaccharides, and their detailed structures were elucidated by their data-dependent MS² spectra.

Figure 7(A) shows the total ion current (TIC) profile obtained by the full MS¹ scan of PA-labeled oligosaccharides from the murine kidney. Structures of major oligosaccharides a–i were deduced from the masses of the sodiated molecular ions measured by FTMS together with the B/Y ions generated by CID MS² (Table 1). Figures 7(B)–7(D) show mass chromatograms at *m/z* 534, 388 and 259, respectively, detected by MS²⁻⁴, respectively. These chromatograms revealed that at least five kinds of oligosaccharides contain the Le^x-motif (a, b, e, f and h). Based on the masses, they were assigned to fucosylated oligosaccharides consisting of dHex₃Hex₅HexNAC₅ (a and f), dHex₂Hex₅HexNAC₅ (b), dHexHex₄HexNAC₅ (e), and dHex₂Hex₄HexNAC₅ (h) (abbreviations used here are: dHex, deoxyhexose; Hex, hexose; HexNAC, *N*-acetylhexosamine).

As an example of structural elucidation, we show the MS²⁻⁴ spectra of oligosaccharide f in Fig. 8. In the MS² spectrum, we can observe the product ion [dHex₂HexHexNAC+Na]⁺ at *m/z* 680, which can be assigned to either the Lewis b (Le^b)- or Lewis y (Le^y)-motif. As shown in Fig. 1, Le^b- and Le^y-motifs contain Le^a and Le^x as partial structures, respectively. The generation of Le^x-diagnostic ions suggests the attachment of the Le^y-motif to oligosaccharide f. Furthermore, product ions at *m/z* 1036 and 446 prove the linkage of GlcNAc at β -mannose in the trimannosyl core structure and fucosylation of the reducing terminal GlcNAc, respectively. Based on these characteristic ions, oligosaccharide f can be assigned to the bisected and fucosylated biantennary bearing the

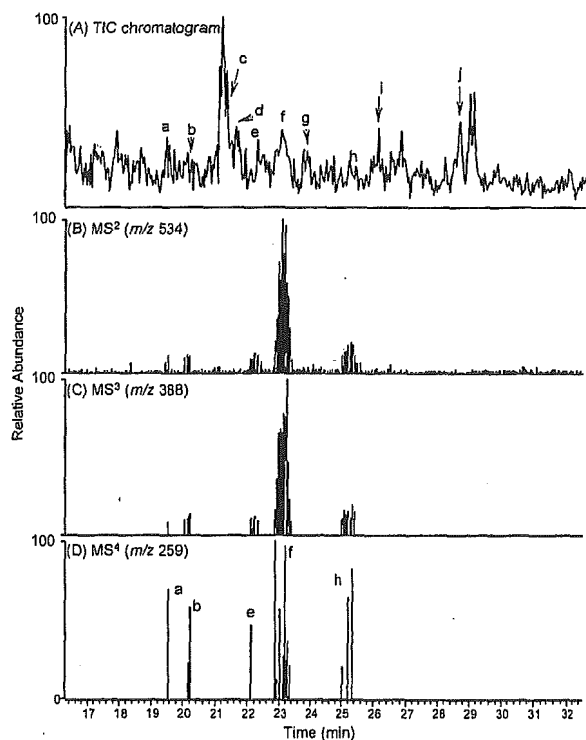


Figure 7. Specific detection of *N*-linked Le^x-oligosaccharides in murine kidney by LC/ESI-MSⁿ: (A) total ion chromatogram obtained by MS¹; (B) mass chromatogram of [dHexHexNAC+Na]⁺ at *m/z* 534 detected in MS²; (C) mass chromatogram of [HexHexNAC+Na]⁺ at *m/z* 388 detected in MS³; and (D) mass chromatogram of the cross-ring fragment at *m/z* 259 detected in MS⁴.

Table 1. Sugar composition and deduced structure of *N*-linked oligosaccharide from murine kidney

Sugar No.	Composition ^a	Deduced structure	Lewis type
a	dHex ₃ Hex ₅ HexNAc ₅		Le ^y
b	dHex ₂ Hex ₅ HexNAc ₅		Le ^x
c	Hex ₈ HexNAc ₂		
d	Hex ₉ HexNAc ₂		
e	dHexHex ₄ HexNAc ₅		Le ^x
f	dHex ₃ Hex ₅ HexNAc ₅		Le ^y
g	Hex ₆ HexNAc ₂		
h	dHex ₂ Hex ₄ HexNAc ₅		Le ^x
i	Hex ₇ HexNAc ₂		
j	Hex ₅ HexNAc ₂		

^aFuc, fucose; Hex, hexose; HexNAc, *N*-acetylhexosamine.

○ Gal; ○ Man; ■ GlcNAc; △ Fuc.

Le^y-motif. The Le^y structure in oligosaccharide f was confirmed by an extra LC/MS² run without post-column reaction with NaCl. Figure 9 shows the MS² spectrum of [M+H+NH₄]²⁺ at *m/z* 1189.4. Attachment of the Le^y-motif was proved by the generation of the product ion at *m/z* 658 corresponding to [dHex₂HexHexNAc]⁺.

Other oligosaccharides were assigned to bisected bian-tennary forms bearing Le^y (oligosaccharide a) and those bearing Le^x (oligosaccharides b, e and h) motifs. In addition to the previously reported Le^x-oligosaccharides,²⁰ we also detected the presence of Le^y-oligosaccharides in the murine kidney.

CONCLUSIONS

We found that the cross-ring fragment ion at *m/z* 259, which can be used for distinction from positional isomers, was generated from Le^x-oligosaccharides by MS⁴ of [GalGlcNAc+Na]⁺ at *m/z* 388, which was generated by MS³ of [Gal(Fuc)GlcNAc+Na]⁺ at *m/z* 534. Then, we successfully detected and elucidated the Le^x- and Le^y-oligosaccharides in the complex mixture using a sequential scan consisting of full MS¹, data-dependent MS², MS³ of the sodiated ion at *m/z* 534, and MS⁴ of the sodiated ion at *m/z* 388.

The Le^x structure is associated with various biological events as oligosaccharide ligands. So far, the detection and structural analyses of Le^x-oligosaccharides have required complicated and time-consuming processes, such as exoglycosidase digestions, sugar mapping,²⁷ the use of lectins and immunological methods. The mass spectrometric method proposed here would enable the rapid and easy detection of the Le^x-motif and subsequent structural elucidation of

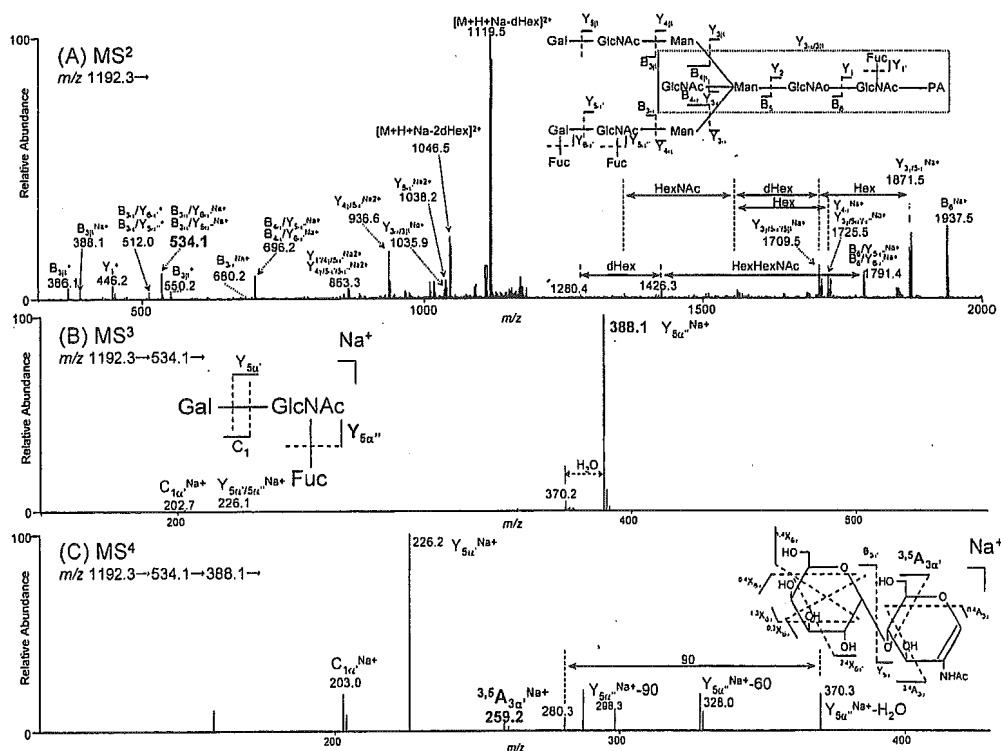


Figure 8. MS²⁻⁴ spectra of oligosaccharide f by LC/ESI-MSⁿ: (A) MS² spectrum of [M+H+Na]²⁺ at *m/z* 1192.3; (B) MS³ spectrum of [dHexHexNAc+Na]⁺ at *m/z* 534.1 detected in MS²; and (C) MS⁴ spectrum of [HexHexNAc+Na]⁺ at *m/z* 388.1 detected in MS³.

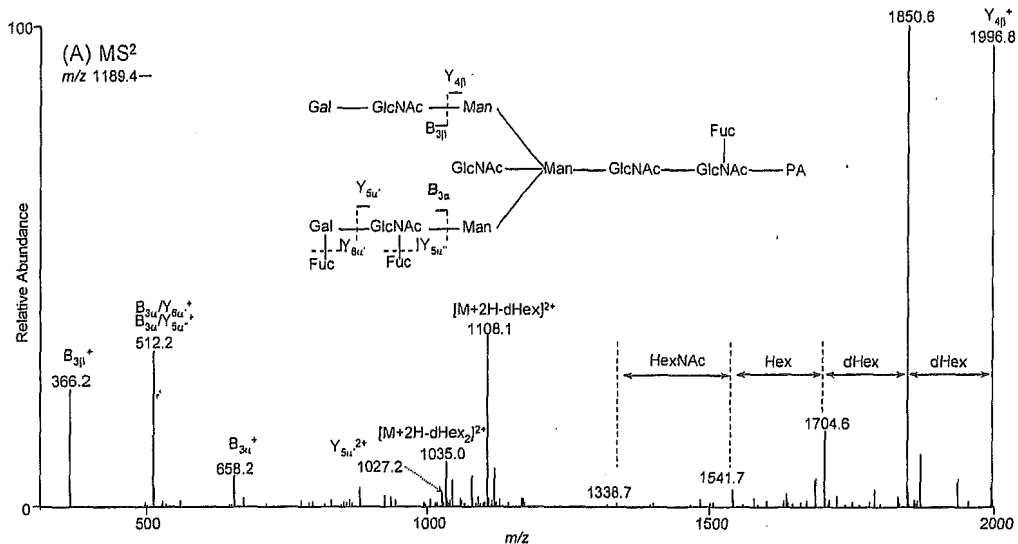


Figure 9. MS² spectrum of oligosaccharide f by LC/ESI-MSⁿ; precursor ion, [M+H+NH₄]²⁺ at m/z 1189.9.

Le^x-oligosaccharides in biological samples. Our method, based on a sequential scan for the structure-characteristic ions, may be applicable to the analyses of oligosaccharides carrying other partial motifs, such as sialyl Le^x and sulfated sugar.

Acknowledgements

This study was supported in part by Grant-in-Aid from the Ministry of Health Labor and Welfare, and Core Research for the Evolutional Science and Technology Program, Japan Science and Technology Corp.

REFERENCES

1. Feizi T. *Nature* 1985; 314: 53.
2. Walz G, Aruffo A, Kolanus W, Bevilacqua M, Seed B. *Science* 1990; 250: 1132.
3. Kannagi R, Izawa M, Koike T, Miyazaki K, Kimura N. *Cancer Sci.* 2004; 95: 377.
4. Coombs PJ, Graham SA, Drickamer K, Taylor ME. *J. Biol. Chem.* 2005; 280: 22993.
5. Larkin M, Ahern TJ, Stoll MS, et al. *J. Biol. Chem.* 1992; 267: 13661.
6. Lowe JB, Stoolman LM, Nair RP, Larsen RD, Berhend TL, Marks RM. *Cell* 1990; 63: 475.
7. Phillips ML, Nudelman E, Gaeta FC, Perez M, Singhal AK, Hakomori S, Paulson JC. *Science* 1990; 250: 1130.
8. Sagi D, Peter-Katalinic J, Conradt HS, Nimtz M. *J. Am. Soc. Mass Spectrom.* 2002; 13: 1138.
9. Sheeley DM, Reinhold VN. *Anal. Chem.* 1998; 70: 3053.
10. Xue J, Song L, Khaja SD, Locke RD, West CM, Laine RA, Matta KL. *Rapid Commun. Mass Spectrom.* 2004; 18: 1947.
11. Karlsson NG, Schulz BL, Packer NH. *J. Am. Soc. Mass Spectrom.* 2004; 15: 659.
12. Karlsson NG, Wilson NL, Wirth HJ, Dawes P, Joshi H, Packer NH. *Rapid Commun. Mass Spectrom.* 2004; 18: 2282.
13. Zhang S, Chelius D. *J. Biomol. Technol.* 2004; 15: 120.
14. Royle L, Mattu TS, Hart E, Langridge JI, Merry AH, Murphy N, Harvey DJ, Dwek RA, Rudd PM. *Anal. Biochem.* 2002; 304: 70.
15. Takegawa Y, Deguchi K, Ito S, Yoshioka S, Nakagawa H, Nishimura S. *Rapid Commun. Mass Spectrom.* 2005; 19: 937.
16. Takegawa Y, Ito S, Yoshioka S, Deguchi K, Nakagawa H, Monde K, Nishimura S. *Rapid Commun. Mass Spectrom.* 2004; 18: 385.
17. Mechref Y, Novotny MV, Krishnan C. *Anal. Chem.* 2003; 75: 4895.
18. Weiskopf AS, Vouros P, Harvey DJ. *Anal. Chem.* 1998; 70: 4441.
19. Meisen I, Peter-Katalinic J, Muthing J. *Anal. Chem.* 2003; 75: 5719.
20. Chui D, Sellakumar G, Green R, Sutton-Smith M, McQuistan T, Marek K, Morris H, Dell A, Marth J. *Proc. Natl. Acad. Sci. USA* 2001; 98: 1142.
21. Yuan J, Hashii N, Kawasaki N, Itoh S, Kawanishi T, Hayakawa T. *J. Chromatogr. A* 2005; 1067: 145.
22. Song F, Cui M, Liu Z, Yu B, Liu S. *Rapid Commun. Mass Spectrom.* 2004; 18: 2241.
23. Cui M, Song F, Liu Z, Liu S. *Rapid Commun. Mass Spectrom.* 2001; 15: 586.
24. Vakhrushev SY, Zamfir A, Peter-Katalinic J. *J. Am. Soc. Mass Spectrom.* 2004; 15: 1863.
25. Suzuki S, Kakehi K, Honda S. *Anal. Chem.* 1996; 68: 2073.
26. Yoshino K, Takao T, Murata H, Shimonishi Y. *Anal. Chem.* 1995; 67: 4028.
27. Tomiya N, Awaya J, Kurono M, Endo S, Arata Y, Takahashi N. *Anal. Biochem.* 1988; 171: 73.



Characterization of a gel-separated unknown glycoprotein by liquid chromatography/multistage tandem mass spectrometry Analysis of rat brain Thy-1 separated by sodium dodecyl sulfate-polyacrylamide gel electrophoresis

Satsuki Itoh^a, Nana Kawasaki^{a,b,*}, Akira Harazono^a, Noritaka Hashii^a,
Yukari Matsuishi^b, Toru Kawanishi^a, Takao Hayakawa^a

^a Division of Biological Chemistry and Biologicals, National Institute of Health Science, 1-18-1, Kamiyoga, Setagaya-ku, Tokyo 158-8501, Japan

^b CREST, Japan Science and Technology Agency (JST), Japan

Received 17 May 2005; received in revised form 17 July 2005; accepted 25 July 2005

Available online 5 October 2005

Abstract

We developed an efficient and convenient strategy for protein identification and glycosylation analysis of a small amount of unknown glycoprotein in a biological sample. The procedure involves isolation of proteins by electrophoresis and mass spectrometric peptide/glycopeptide mapping by LC/ion trap mass spectrometer. For the complete glycosylation analysis, proteins were extracted in intact form from the gel, and proteinase-digested glycoproteins were then subjected to LC/multistage tandem MS (MSⁿ) incorporating a full mass scan, in-source collision-induced dissociation (CID), and data-dependent MSⁿ. The glycopeptides were localized in the peptide/glycopeptide map by using oxonium ions such as HexNAc⁺ and NeuAc⁺, generated by in-source CID, and neutral loss by CID-MS/MS. We conducted the search analysis for the glycopeptide identification using search parameters containing a possible glycosylation at the Asn residue with *N*-acetylglucosamine (203 Da). We were able to identify the glycopeptides resulting from predictable digestion with proteinase. The glycopeptides caused by irregular cleavages were not identified by the database search analysis, but their elution positions were localized using oxonium ions produced by in-source CID, and neutral loss by the data-dependent MSⁿ. Then, all glycopeptides could be identified based on the product ion spectra which were sorted from data-dependent CID-MSⁿ spectra acquired around localized positions. Using this strategy, we successfully elucidated site-specific glycosylation of Thy-1, glycosylphosphatidylinositol (GPI)-anchored proteins glycosylated at Asn23, 74, and 98, and at Cys11. High-mannose-type, complex-type, and hybrid-type oligosaccharides were all found to be attached to Asn23, 74 and 98, and four GPI structures could be characterized. Our method is simple, rapid and useful for the characterization of unknown glycoproteins in a complex mixture of proteins.
© 2005 Elsevier B.V. All rights reserved.

Keywords: Glycoprotein; LC/MS; Ion trap mass spectrometer; In-source CID; Thy-1

1. Introduction

Glycosylation is one of the most abundant post-translational modifications of proteins [1]. Most glycoproteins exist in heterogeneous forms due to their carbohydrate heterogeneity at multiple glycosylation sites. Because heterogeneity at each glycosylation site can be associated with

many biological functions [2,3], it is necessary to analyze the oligosaccharide structures at each glycosylation site.

Mass spectrometric peptide/glycopeptide mapping by liquid chromatography coupled with electrospray ionization tandem mass spectrometry (LC/ESI-MS/MS) is now used for characterization of glycoproteins [4,5]. Site-specific glycosylation of some gel-separated glycoproteins can be analyzed by in-gel proteinase digestion followed by MS; this method, however, gives unsatisfactory results due to a lower recovery of some glycopeptides from the gel [6–8]. For

* Corresponding author. Tel.: +81 3 3700 1141; fax: +81 3 3707 6950.
E-mail address: nana@nihs.go.jp (N. Kawasaki).

complete site-specific glycosylation analysis, all glycopeptide fragments should be recovered from the gel. Hence, the extraction of a whole glycoprotein from the gel before proteinase digestion would be more reasonable than in-gel digestion. Additionally, the poor ionization efficiency of glycopeptides makes it difficult to analyze the glycosylation of glycopeptides in a complex mixture of peptides [6,9]. The glycopeptide-specific method is required for mass spectrometric peptide/glycopeptide mapping.

A precursor ion scan using triple quadrupole-type mass spectrometer is favorably used for analysis of glycopeptides [10–13]. However, this method requires repetitive analysis for the protein identification and glycosylation analysis, as it monitors carbohydrate marker ions such as HexNAc⁺ and Hex-HexNAc⁺ fragmented from glycopeptides by collision-induced dissociation (CID)-MS/MS, and does not provide product ion spectra of non-glycosylated peptides. As such, additional analysis would not be possible for small quantities of proteins, including gel-separated glycoproteins. As an alternative method, we have previously demonstrated peptide/glycopeptide mapping using quadrupole time-of-flight mass spectrometer, by which product ions arise from both peptides and carbohydrates [14]. Using oxonium ions as marker ions, we can sort out product ion spectra of glycopeptides from a number of product ion spectra of peptides, and can determine the amino acid sequences of glycopeptides, glycosylation sites, and monosaccharide composition in a single analysis. Recently, ion trap mass spectrometry (ITMS), which is capable of data-dependent multistage tandem MS (MSⁿ), has been found to be preferable for use in glycosylation analysis of glycopeptides [15,16]. Glycopeptide-specific detection by precursor ion scan and data-dependent scan cannot be used for glycosylation analysis by ITMS due to the low mass cut-off system. Instead, oxonium ions fragmented by in-source CID are used for the localization of glycopeptides in the peptide/glycopeptide map [3,17]. It has recently been reported that peptide + GlcNAc ions originating from *N*-glycosylated peptides by MS² yield peptide b and y ions by further MSⁿ, and that the peptide sequence and *N*-glycosylation sites can be identified based on the peptide fragment ions [15,16,18]. In addition, another group has reported that glycopeptides can be identified in peptide/glycopeptide map by a search analysis using a database to which all possible cleavage products of the glycopeptides have been added in advance [19]. A combination of peptide/glycopeptide mapping with in-source CID, data-dependent CID-MSⁿ, and the database search analysis would enable protein identification, glycopeptide selection, and glycosylation analysis of a small amount of glycoprotein.

In the present study, we developed a strategy for the characterization of a small amount of unknown glycoprotein in a biological sample. An unknown glycoprotein was isolated by electrophoresis and extracted from the gel in an intact form. We used sodium dodecyl sulfate (SDS), which is effective for extracting proteins from the gel, and could be easily removed by adding cold acetone. The proteinase-

digested glycoprotein was subjected to peptide/glycopeptide mapping, with the sequential scan consisting of a full mass scan, in-source CID, and data-dependent CID-MSⁿ. Using this method, we carried out site-specific glycosylation analysis of glycosylphosphatidylinositol (GPI)-anchored proteins in rat brain. A computer database search was used for the identification of a GPI-anchored protein and its *N*-glycosylation sites. In-source CID and data-dependent CID-MS/MS were also used for localization of peptides with *N*-glycan and GPI in the peptide/glycopeptide map. On the basis of their product ion spectra, we elucidated *N*-glycosylation at each glycosylation site and the structure of GPIs.

2. Experimental

2.1. Materials

Rat brains were purchased from Nippon SLC (Hamamatsu, Japan). Trypsin-Gold and endoproteinase Asp-N were purchased from Promega (Madison, WI, USA) and Wako Pure Chemical (Osaka, Japan), respectively. Phosphatidylinositol-specific phospholipase C (PIPLC) from *Bacillus cereus* were purchased from Molecular Probes (Eugene, OR, USA). All other chemicals used were of the highest purity available.

2.2. Sodium dodecyl sulfate-polyacrylamide gel electrophoresis (SDS-PAGE) of PIPLC-treated GPI-anchored proteins

PIPLC-treated GPI-anchored proteins were prepared from rat brain utilizing Triton X-114 phase partition and PIPLC digestion [20,21]. Two whole rat brains (2.8 g, Wistar, male, 3 weeks) were homogenized in cold acetone and centrifuged for 10 min at 4 °C. The precipitate was then homogenized in CHCl₃: methanol (2:1, v/v) and centrifuged for 10 min at 4 °C. After being washed with methanol, the pellet was homogenized in 50 mM Tris-HCl (pH 7.4) containing 150 mM NaCl, 1 mM ethylenediaminetetraacetic acid (EDTA), and 1 mM phenylmethylsulfonyl fluoride (PMSF), and centrifuged at 10,000 × *g* at 4 °C for 20 min. The pellet was resuspended in the same buffer with an additional 2% Triton X-114 (v/v), and stirred at 4 °C for 16 h. After centrifugation at 10,000 × *g* at 4 °C for 20 min, the supernatant was subjected to Triton X-114 phase-partitioning at 37 °C for 10 min. The detergent phase was resuspended with an equal volume of 50 mM Tris-HCl (pH 7.4) containing 150 mM NaCl. Solubilized membrane proteins in the detergent phase were precipitated with cold acetone and were resuspended in 400 μl of 50 mM Tris-HCl (pH 7.4). Following the addition of PIPLC (1 U), the suspension was incubated at 37 °C for 18 h. The suspension was resubjected to Triton X-114 phase-partitioning, and PIPLC-treated GPI-anchored proteins were precipitated with cold acetone from the aqueous phase. PIPLC-treated GPI-anchored proteins obtained from

50 mg of rat brain were separated by SDS-PAGE (12.5%) after carboxyamidomethylation [22].

2.3. Extraction and digestion of gel-separated proteins

The protein in gel band was extracted with 20 mM Tris-HCl containing 1% SDS by shaking vigorously overnight after breaking down the gel into small bits. The extract was filtered with Ultrafree-MC (0.22 μ m, Millipore, Bedford, USA), and the protein was precipitated by adding cold acetone. The precipitate was digested with trypsin (1 μ g) in 20 μ l of 0.1 M Tris-HCl (pH 8.0) at 37 °C for 16 h, or with Asp-N (0.4 μ g) in 20 μ l of 5 mM Tris-HCl (pH 7.5) at 37 °C overnight.

2.4. LC/MSⁿ

Proteolytic peptides were separated by a Magic C18 column (50 mm \times 0.2 mm, 3 μ m, Michrom BioResources, Auburn, CA, USA) with a Paradaim MS4 HPLC system (Michrom BioResources Inc., Auburn, CA, USA) consisting of pump A: 0.1% formic acid and 2% acetonitrile, and pump B: 0.1% formic acid and 90% acetonitrile. Separation was performed with a linear gradient of 5–65% of pump B in 40 min after 5% in 10 min of pump B at a flow rate 3 μ l/min. Mass spectra were recorded by Finnigan LTQ (Thermo Electron, San Jose, CA, USA) with the sequential scan: a full mass scan (m/z 300–2000), a full mass scan with in-source CID (m/z 80–500, collision energy: 50 V), and data-dependent CID-MSⁿ for most intense ions at each scan with dynamic exclusion for 30 s. Scan time (m/z 300–2000) is approximately 0.1 s. The operating condition used for LC/ITMS was as follows: tube lens offset of 130 V, capillary voltage of 2.0 kV, capillary temperature of 200 °C.

2.5. Computer database search analysis

All product ions obtained by LC/ITMS were subjected to the computer database search analysis with the TurboSEQUEST search engine (Thermo Electron, San Jose, CA, USA). We used the NCBI database (rat, updated at February 2003) and following search parameters: a static modification of carboxyamidomethylation (57 Da) at Cys, a possible modification of GlcNAc (203 Da) at Asn, and trypsin used for digestion.

3. Results

3.1. Extraction of whole proteins from the gel

Rat brain PIPLC-treated GPI-anchored proteins were separated by SDS-PAGE (Fig. 1), and the most noticeable band at 20–25 kDa was cut off from the gel and crushed. The gel pieces were shaken vigorously in 1% SDS, and the extracted protein was precipitated with cold acetone to remove SDS.

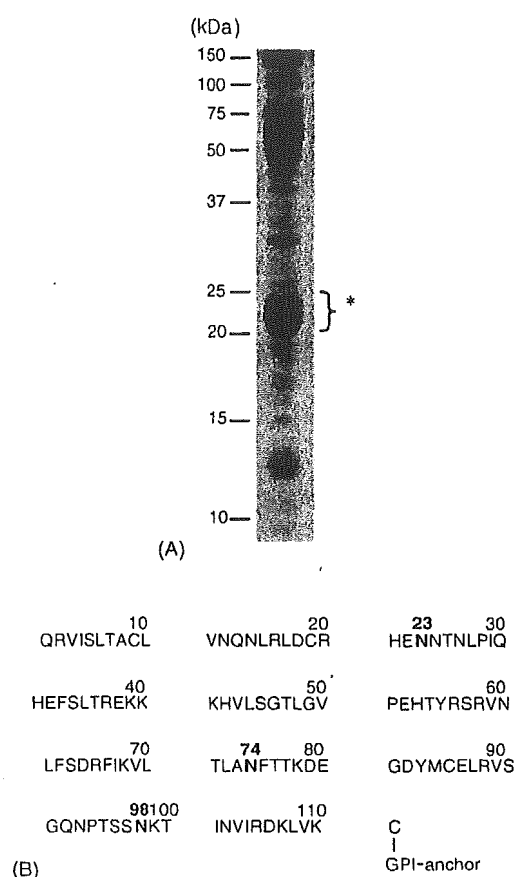


Fig. 1. (A) SDS-PAGE of PIPLC-treated GPI-anchored proteins from rat brain. (B) Amino acid sequence of rat Thy-1. *N*-Glycosylation sites are indicated by bold face. The protein at 20–25 kDa indicated by asterisk was subjected to the glycosylation analysis in this study.

We checked the recovery of the protein at 20–25 kDa by comparing the fluorescence intensity (Ex 633 nm/Em 670 nm) of the proteins at 20–25 kDa visualized by Coomassie staining before and after extraction. Approximately 55% of the protein at 20–25 kDa could be recovered from the gel (data not shown). The protein was digested with trypsin and subjected to the sequential scan consisting of full mass scans with and without in-source CID and data-dependent MSⁿ by LC/ITMS for protein identification and glycosylation analysis.

3.2. Database search analysis

Fig. 2(A) shows the peptide/glycopeptide map of the trypsin-digested protein at 20–25 kDa. First, all product ions generated by data-dependent MSⁿ were used for the database search analysis. Using search parameters described in Section 2.5, the protein was identified as Thy-1, a glycoprotein containing three *N*-glycosylation sites at Asn23, 74, and 98, and a GPI attachment site at Cys111. The search analysis also suggested the glycosylation at Asn74 and 98, with elution positions of 34 min (peak T6, Val69-Lys78) and 3.5 min (peak T1, Val89-Lys99), respectively (Fig. 2(A)). Although

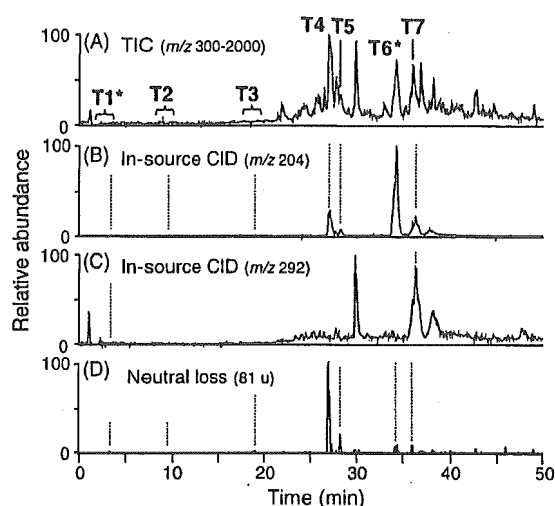


Fig. 2. Total ion chromatogram (TIC) of trypsin-digested protein at 20–25 kDa (m/z 300–2000) (A), mass chromatograms from TIC with ion-source CID of m/z 204 (B) and 292 (C), and neutral loss chromatogram of 81 u by data-dependent CID-MS/MS (D). Asterisks mean the peak of glycopeptides identified by the database search analysis.

the glycopeptide Val89-Lys99 contains two Asn residues, Asn93 and 98, only Asn98 was identified as a glycosylation site because of detection of b and y ions modified with GlcNAc at Asn98.

Next, to study the site-specific glycosylation at Asn74 and 98, product ion spectra of glycopeptides were sorted from the numbers of product ion spectra acquired around peak T6 and T1. We sorted out product ion spectra of glycopeptides using B series ions, such as $\text{Hex}_1\text{HexNAc}_1^+$ and $\text{Hex}_2\text{HexNAc}_1^+$ (m/z 366 and 528) originated from glycopeptides by CID-MS/MS, as marker ions [23]. We could sort out 14 product ion spectra originated from glycopeptide Val69-Lys78 around peak T6. The monosaccharide compositions of *N*-glycans at Val69-Lys78 were calculated as $\text{dHex}_{0-3}\text{Hex}_{2-7}\text{HexNAc}_{2-5}$ on the basis of the m/z values of their molecular ions and the theoretical mass of the peptide. Likewise, seven product ion spectra originated from glycopeptide Val89-Lys99 were sorted from those around peak T1, and their monosaccharide compositions were estimated as $\text{dHex}_{0-2}\text{Hex}_{3,5,6}\text{HexNAc}_{2-5}\text{NeuAc}_{0,1}$ (Table 1). Glycosylation at Asn74 and 98 were elucidated by a detailed examination of these product ion spectra as follows.

3.2.1. Analysis of the glycosylation at Asn74 of peptide Val69-Lys78

Fig. 3(A) shows a product ion spectrum of the glycopeptide Val69-Lys78 at 34.52 min. Its precursor ion is the doubly charged ion at m/z 1512.2. Many product ions generated by cleavages of glycosidic linkages can be observed in this product ion spectrum. The most intense ion at m/z 1311 is assigned to a peptide bearing the reducing end of GlcNAc, which was caused by glycosidic linkage cleavage of *N*-linked

oligosaccharide. Fig. 3(B) is the product ion spectrum of the peptide + GlcNAc ion at m/z 1311. The b and y ions generated by cleavages of the peptide backbone prove that this glycopeptide is the peptide Val69-Lys78 glycosylated at Asn74.

The molecular weight of the carbohydrate moiety can be calculated as 1933.8 Da by subtracting the theoretical mass of the peptide (1106.6 Da) from the calculated glycopeptide mass (3022.4 Da). Consequently, the monosaccharide composition can be estimated as $\text{dHex}_2\text{Hex}_5\text{HexNAc}_4$. In the product ion spectrum (Fig. 3(A)), B ions corresponding to $\text{dHex}_1\text{Hex}_1\text{HexNAc}_1$ ($\text{B}_{2\alpha}$) and $\text{dHex}_1\text{Hex}_2\text{HexNAc}_1$ ($\text{B}_{3\alpha}$) were detected at m/z 512 and 674, respectively. These results indicate that one of two dHex, which are likely to be Fuc, attaches to Gal-GlcNAc at the non-reducing end in a similar manner as the Lewis a/x antigen (Gal-(Fuc-)GlcNAc-), or the blood group H-determinant (Fuc-Gal-GlcNAc-). The product ion at m/z 350 produced from the triply charged precursor ion at m/z 1008.7 corresponded to $\text{dHex}_1\text{HexNAc}_1$ (data not shown), suggesting that Fuc attaches to GlcNAc like the Lewis a/x antigen (Gal-(Fuc-)GlcNAc-). The attachment site of the other Fuc can be deduced at inner trimannosyl core GlcNAc from the observation of Y ions at m/z 1457, 1660, and 1822, which correspond to Val69-Lys78 plus $\text{dHex}_1\text{HexNAc}_1$ ($\text{Y}_{1\alpha}$), $\text{dHex}_1\text{HexNAc}_2$ ($\text{Y}_{2\alpha}$), and $\text{dHex}_1\text{Hex}_1\text{HexNAc}_2$ ($\text{Y}_{3\alpha/3\beta/3\gamma}$), respectively. In addition, the product ion at m/z 1411 resulting from the precursor ion at m/z 1512.2 by loss of 101.6 u (HexNAc), suggests a linkage of non-substituted HexNAc at the non-reducing terminal end. Together with detection of the product ion at m/z 940 ($\text{Y}_{3\alpha/1\beta/3\beta}^+$, $[\text{GlcNAc-Man-GlcNAc-GlcNAc-peptide+H}]^{2+}$), it can be deduced that this HexNAc is a bisecting GlcNAc attached to the core mannose residue via a β 1–4 linkage. From these product ions, we could deduce two oligosaccharide structures. One is the structure indicated in Fig. 3(A), inset, and the other is one containing a Gal-Gal-(Fuc-)GlcNAc-Man-branch instead of a Gal-(Fuc-)GlcNAc-Man-branch. Detection of Gal-(Fuc-)GlcNAc-Man⁺ at m/z 674 but not Gal-Gal-(Fuc-)GlcNAc-Man⁺ at m/z 836 suggests that this oligosaccharide structure can be assigned to the structure indicated in Fig. 3(A), inset.

The carbohydrate structures of the other glycopeptide Val69-Lys78 detected around peak T6 can be characterized as the high-mannose-type oligosaccharide (M5), complex-type oligosaccharides containing some partial structures such as inner core Fuc, bisecting GlcNAc, the Lewis a/x antigen, and blood group H-determinant, and hybrid-type oligosaccharides (Table 1).

3.2.2. Analysis of the glycosylation at Asn98 of peptide Val89-Lys99

Fig. 4 shows one of the product ion spectra of the glycopeptide Val89-Lys99 at 3.47 min. Its precursor ion is the doubly charged ion at m/z 1525.8. The monosaccharide composition, $\text{dHex}_1\text{Hex}_6\text{HexNAc}_4$, can be estimated based on the calculated mass of the carbohydrate moiety (1950.0 Da) obtained by subtracting the mass of the theo-

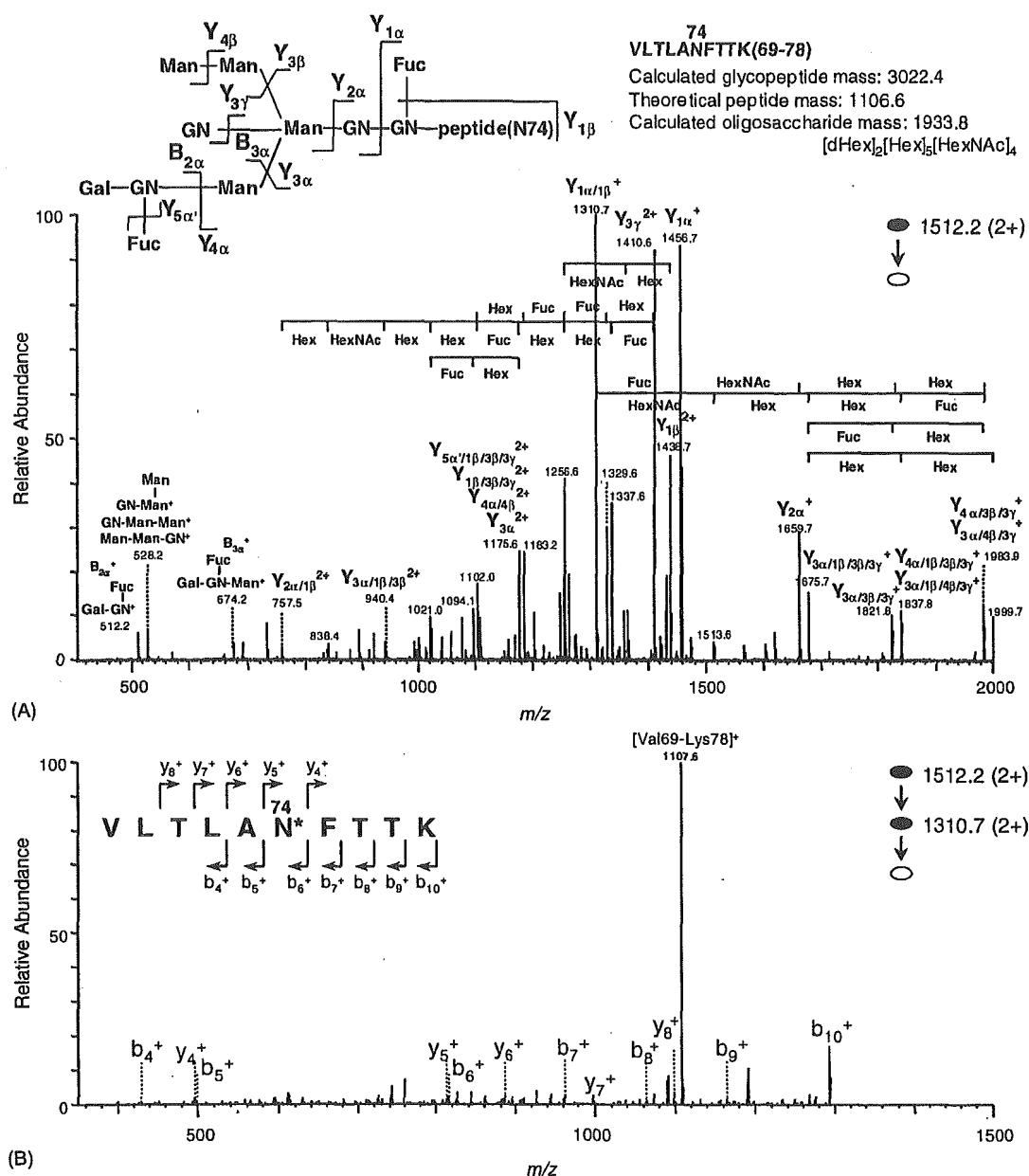


Fig. 3. (A) Product ion spectrum (MS^2) of the doubly charged glycopeptide precursor ion at m/z 1512.2 in peak T6. The glycopeptide Val69-Lys78 is glycosylated with oligosaccharide, $dHex_2Hex_5HexNAC_4$ at Asn74, and the inset is the deduced oligosaccharide structure. (B) MS^3 product ion spectrum derived from the doubly charged glycopeptide precursor ion at m/z 1512.2, followed by further fragmentation of the product ion at m/z 1310.7.

retical typtic peptide mass (1117.5 Da) from the calculated glycopeptide mass (3049.5 Da). Y ions corresponding to Val89-Lys99 plus $dHex_1HexNAC_1$ ($Y_{1\alpha}$), $dHex_1HexNAC_2$ ($Y_{2\alpha}$), and $dHex_1Hex_1HexNAC_2$ ($Y_{3\alpha/3\beta/3\gamma}$) detected at m/z 1468, 1671, and 1833, respectively, reveals that one Fuc residue is linked to the inner trimannosyl core GlcNAc. Additionally, the product ion at m/z 1424 suggests a linkage of non-substituted HexNAc at the non-reducing terminal end. Together with the product ions at m/z 945 and 1890, it can be deduced that this HexNAc is a bisecting GlcNAc that attaches

to a core mannose residue via a β 1–4 linkage. On the basis of the product ions at m/z 487, 528 and 1380, corresponding to Hex_3 ($B_{2\beta}$), $Hex_2HexNAC_1$ ($B_{3\alpha}$), and $Hex_6HexNAC_2$ ($B_{4\alpha}$), the oligosaccharide structure was characterized as a hybrid-type oligosaccharide (Fig. 4, inset).

The carbohydrate structures of the other glycopeptide Val89-Lys98 detected around peak T1 are characterized as high-mannose-type oligosaccharide (M5), complex-type, and hybrid-type oligosaccharides, which include bisecting GlcNAc and Lewis a/x structures (Table 1).

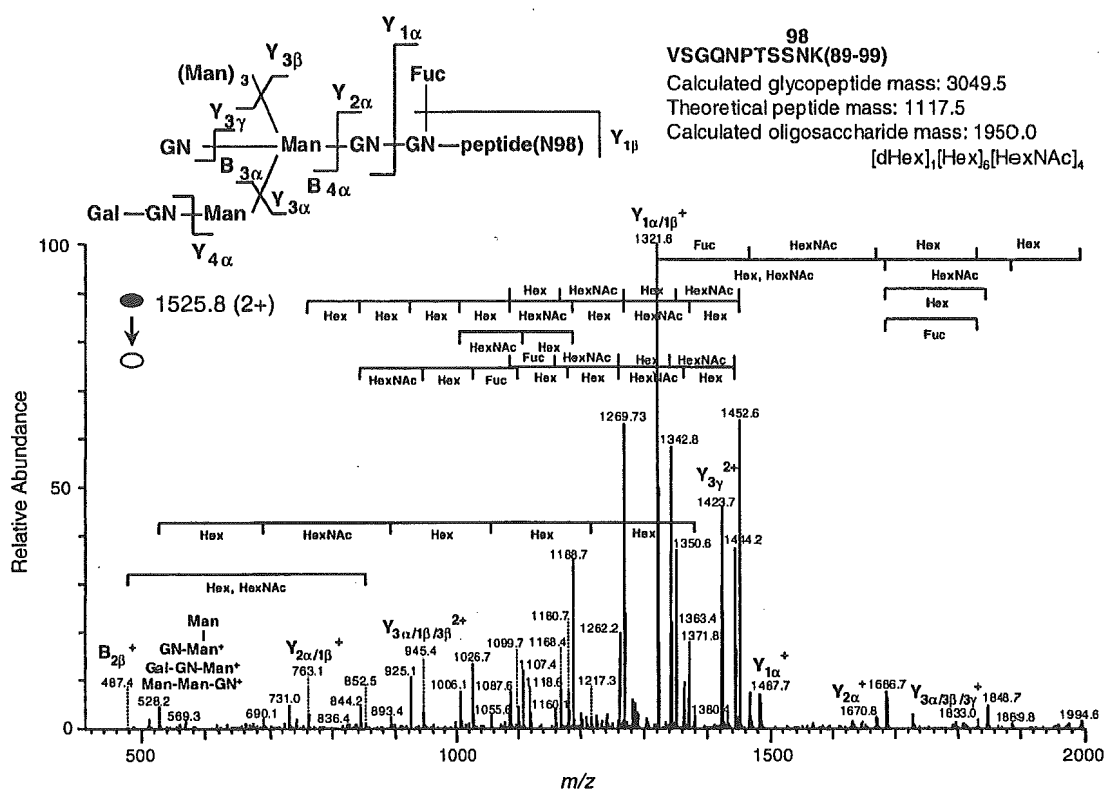


Fig. 4. Product ion spectrum of the doubly charged glycopeptide precursor ion at m/z 1525.8 in peak T1. The glycopeptide Val89-Lys99 is glycosylated with the oligosaccharide, dHex₁Hex₆HexNAc₄ at Asn98, and the inset is the deduced oligosaccharide structure.

3.3. Detection of glycopeptides by in-source CID and CID-MS/MS

Glycopeptides containing Asn23 could not be identified by the database search analysis. Therefore, we first localized all glycopeptides in the peptide/glycopeptide map using oxonium marker ions generated by in-source CID. Fig. 2(B and C) shows mass chromatograms of oxonium marker ions, HexNAc⁺ (m/z 204) and NeuAc⁺ (m/z 292), respectively. The mass chromatogram of m/z 204 indicates that the glycopeptides were localized around 3.7, 9.7, 19.1, 27.2, 28.4, 34.3, 36.3, and 37.8 min. The mass chromatogram of m/z 292 suggests that the glycopeptides bearing NeuAc were localized around 3.7, 30.0, 36.4, and 38.2 min. In addition to the localization of glycopeptides by in-source CID, we monitored neutral loss caused by data-dependent CID-MS/MS. The neutral loss chromatogram of 81 u indicates the localization of doubly charged glycopeptides ions with Hex at the non-reducing ends. The elution positions of the localized glycopeptides by neutral loss are almost identical to those by in-source CID. Second, for confirmation of the elution position of glycopeptides and characterization of the carbohydrate moiety, we sorted the product ion spectra of glycopeptides from enormous numbers of data-dependently acquired product ion spectra around localized glycopeptides by using oligosaccharide oxonium ions as marker ions. Consequently, the locations of glycopeptides were confirmed

in peak T1-6 (Fig. 2(A)). The peaks T1 and 6 correspond to the location of glycopeptides identified by the database search as Val89-Lys99 and Val69-Lys78, respectively. Four glycopeptide peaks were newly sorted by in-source CID and data-dependent CID-MS/MS. Structural assignment of the glycopeptides in these peaks was carried out using their MSⁿ spectra as follows.

3.3.1. Analysis of the glycosylation at Asn23 of peptide His21-Phe33

Fig. 5(A) shows one of the product ion spectra of the glycopeptide His21-Phe33 in peak T4. Its precursor ion is the triply charged ion at m/z 937.3. The intense product ion at m/z 899 is assigned to a doubly charged ion of peptide plus GlcNAc on the basis of Y series ions. The region of His21-Phe33 containing Asn23 in Thy-1 was suggested as the peptide moiety of this glycopeptide, 1593.3 Da, by the FindPept tool available on the internet (ExpASY Proteomics tools, Swiss Institute of Bioinformatics, <http://us.cxpasy.org/tools/findpept.html>). We examined the data-dependently acquired product ion spectrum of the precursor ion at m/z 899 and found that the m/z values of b and y ions in the product ion spectrum were identical to those of predictable product ions originating from the peptide His21-Phe33 modified with HexNAc at Asn23 (Fig. 5(B)). From the calculated oligosaccharide mass (1235.1 Da) obtained by subtracting the theoretical typtic

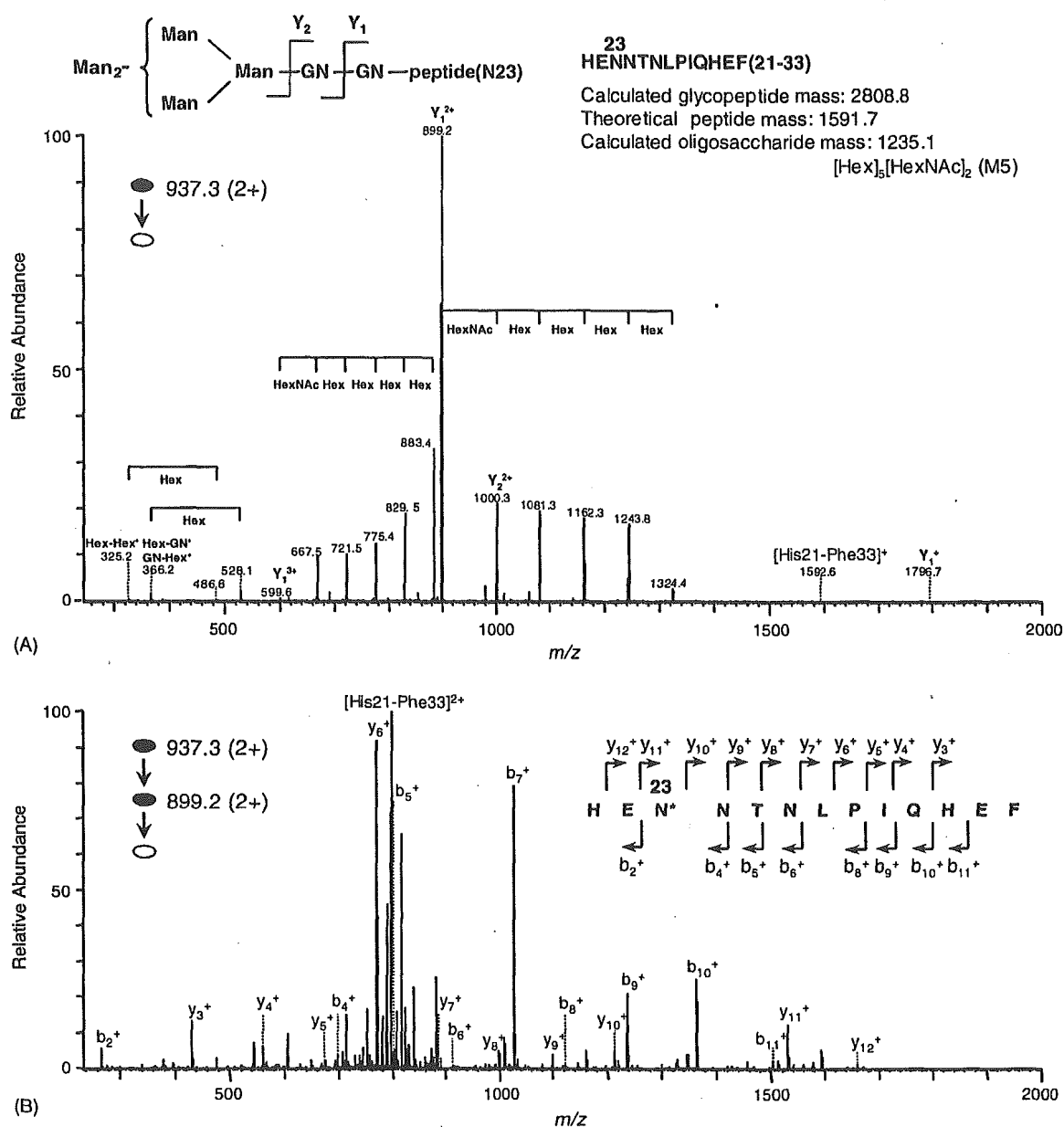


Fig. 5. (A) Product ion spectrum (MS^2) of the doubly charged glycopeptide precursor ion at m/z 937.3 in peak T4. The glycopeptide His21-Phe33 is glycosylated with oligosaccharide, $Hex_5HexNAc_2$ at Asn23, and the inset is the deduced oligosaccharide structure. (B) MS^3 product ion spectrum derived from a doubly charged glycopeptide precursor ion at m/z 937.3, followed by further fragmentation of the product ion at m/z 899.2.

peptide mass (1591.7 Da) from the calculated glycopeptide mass (2808.8 Da) together with product ions at m/z 366 and 528, it is indicated that this peptide carries $Hex_5HexNAc_2$, i.e. high-mannose-type oligosaccharide, M5. All product ion spectra in peak T4 revealed that peptides His21-Phe33 contain only high-mannose-type oligosaccharide (M5).

3.3.2. Analysis of glycopeptides in peaks T2, 3, 5, and 7

Similarly, product ion spectra of glycopeptides around peaks T2, 3, 5, and 7 were sorted by using oligosaccharide

oxonium marker ions generated by MS/MS. In product ion spectra sorted out from around peak T2, the intense ion at m/z 884 was detected and assigned to a singly charged ion of a peptide plus GlcNAc. The peptide was suggested to be Ala73-Lys78 containing Asn74 by the FindPept tool. The monosaccharide composition can be estimated from the calculated mass of oligosaccharide moiety obtained by subtracting the theoretical mass of Ala73-Lys78 (680.35 Da) from calculated glycopeptide mass. Oligosaccharide structure of the glycopeptides is characterized based on their product